Journal of Seismology (2006) **10:** 163–170
DOI: 10.1007/s10950-006-9013-3

The April 9, 2001 Juan Fernández Ridge (M_w 6.7) tensional outer-rise earthquake and its aftershock sequence

R. Fromm[1,†], P. Alvarado[1,2,*], S.L. Beck[1] & G. Zandt[1]
[1]*Department of Geosciences, University of Arizona, 1040E Fourth Street, Tucson AZ 85721, USA*
[2]*Departamento de Geofísica y Astronomía, Universidad Nacional de San Juan, Meglioli 1160 S Rivadavia, San Juan, Argentina*
[*]*Author for correspondence: e-mail: alvarado@geo.arizona.edu*

Received 25 March 2004; accepted in revised form 18 November 2005

Key words: outer-rise, subduction, ridge

Abstract

On April 9, 2001 a M_w 6.7 earthquake occurred offshore of the Chilean coast close to the intersection of the subducting Juan Fernández Ridge (JFR) and the trench near 33°S. The mainshock as well as an unprecedented number of aftershocks were recorded on regional broad-band and short-period seismic networks. We obtained a regional moment tensor solution of the mainshock that indicates a tensional focal mechanism consistent with the Harvard CMT solution. Based on waveform modeling and relocation, the depth of the mainshock was found to be 10–12 km. We relocated 142 aftershocks, which are strongly clustered and restricted to 10–30 km in depth. The seismicity distribution indicates a conjugate normal fault system extending into the lithospheric mantle that correlates with ridge-parallel fractures observed by previous seismic and bathymetric surveys. In conjunction with the historic regional distribution of outer-rise and large interplate seismicity, our results indicate that, with the exception of anomalously large thrust events, preexisting fractures associated with large bathymetric features like ridges have to exist to allow the generation of outer-rise seismicity along the Chilean margin. Hence, flexural bending and time-dependent interplate earthquakes can locally affect the nucleation of outer-rise events. The occurrence of the outer-rise seismicity in the oceanic mantle suggests the existence of lithospheric scale faults which might act as conduits to hydrate the subducting slab.

Introduction

Earthquakes occurring in the seaward extending topographic bulge associated with the flexure of a subducting plate (thus called outer-rise events) are of interest because they are related to the stress-state associated with the change of dip of subduction near the trench. A detailed study of the distribution of outer-rise seismicity provides important constraints on lithospheric rheology, local deformation and interplate coupling (Chapple and Forsyth, 1979; Christensen and Ruff, 1988; Lay et al., 1989; Mueller et al., 1996a, 1996b). A global survey of outer-rise seismicity reveals a large number of extensional events that appear to systematically occur at shallower depths than the relatively few compressional events (Christensen and Ruff, 1988). It has long been recognized that the normal fault seismicity is associated with tensional bending stresses in the upper layer of the subducting plate (Stauder, 1968a, 1968b; Kanamori, 1971; Chapple and Forsyth, 1979; Christensen and Ruff, 1983). The much smaller number of compressional events have been attributed to the compressional bending stresses underneath a neutral stress level (Chapple and Forsyth, 1979; Forsyth, 1982) or to the temporal in-plane loading of the outer-rise

[†]Robert Fromm-Rhim passed away July 31st, 2004.

caused by the locking of the interplate interface prior to large subduction thrust events (Christensen and Ruff, 1983; Christensen and Ruff, 1988). It has recently been recognized that fracture systems associated with large bathymetric features like ridges or seamounts weaken the subducting lithosphere and locally influences the effective rheology and stress state in the vicinity of the trench (von Huene et al., 1997; Flueh et al., 1998; Kopp et al., 2004) and might be an important factor controlling the nucleation of some outer-rise seismicity.

On April 9, 2001 a magnitude M_w 6.7 outer-rise event occurred offshore of the Chilean coast at a latitude of ∼33°S. In this region, the Nazca plate subducts with a velocity of 6.3 cm/yr and an azimuth of 80° underneath the South American plate (Brooks et al., 2003). Moreover, the Juan Fernández Ridge (JFR), defined by a linear chain of unevenly distributed volcanic domes created by hot-spot related magmatic activity (von Huene et al., 1997; Yañez et al., 2001), subducts in this region. Recent local seismic and high-resolution bathymetric surveys reveal the existence of a characteristic ridge-parallel seafloor fabric (von Huene et al., 1997; Flueh et al., 1998; Kopp et al., 2004), which has been interpreted as syngenetic normal faulting associated with the building of the seamounts (Yañez et al., 2001; Kopp et al., 2004).

In this paper we present the results of a study of the 9 April 2001 earthquake, which is the first large outer-rise event in the region for which a large number of aftershocks have been recorded. The event was recorded by regional permanent seismic stations and on a temporary broadband seismic network, which allowed us to obtain a moment tensor solution using regional waveform modeling of the main event together with a detailed aftershock relocation analysis. The presence of the JFR nearby the mainshock epicenter permits us to discuss the potential effect of subducting ridges on the nucleation of outer-rise seismicity.

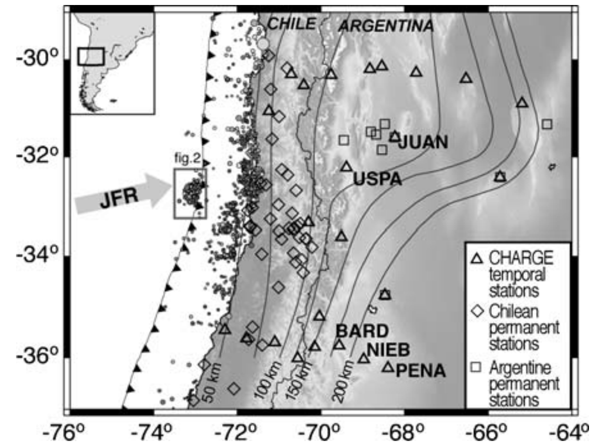

Figure 1. Regional map of the offshore seismicity that occurred during January 2001 and May 2002 as listed by the International Seismological Centre (ISC). Note the concentration of outer-rise events around 33°S close to the intersection of the Juan Fernández Ridge (JFR) and the trench. Location of the seismic stations of the three operating networks are shown with open symbols. Labeled stations, which operated with STS2 sensors, were used in the waveform inversion. Black lines correspond to depths of the top of the subducted slab given by Cahill & Isacks (1992).

Data

The earthquake on 9 April 2001 and its aftershocks were recorded by the permanent seismic networks managed by the Seismological Service of the University of Chile and the Instituto Nacional de Prevención Sísmica (INPRES) in Argentina as well as on a temporary broadband IRIS/PASSCAL network consisting of 22 stations (Figure 1). The temporary broadband network was deployed as part of the CHile Argentina Geophysical Experiment (CHARGE) project to study the transition zone from flat to normal subduction segments around 33°S. In total, over 250 events are included in the International Seismological Centre (ISC) catalog during the CHARGE network operation (January 2001 to May 2002) in the outer-rise region outlined by the gray box in Figure 1 and shown in more detail in Figure 2. Also shown is the largest event ever to occur in this region on 16 October 1981 (M_w 7.2), which is located 70 km south of the 2001 event. This event was found to have a compressional source mechanism with reported depths at 20–40 km (Christensen and Ruff, 1985; Honda et al., 1990; Tichelaar et al., 1992).

The events of the ISC catalog shown in Figures 1 and 2 (including the aftershocks of the 2001 earthquake) are plotted as a function of time in Figure 3. The region becomes seismically active during limited periods of time, not all of them associated with large earthquakes. However, a potential bias due to the lack of network coverage though time cannot be ruled out. With the exception of the 1981 event (which has no recorded aftershocks in the ISC data set), no event of magnitude larger than 5.0 had been recorded until the 2001 event. Only small events ($M < 4$) can be traced back 2 or 3 years before the large 2001 earthquake. We have used the ISC travel time picks and the CHARGE regional broadband waveforms to study this important outer-rise earthquake sequence.

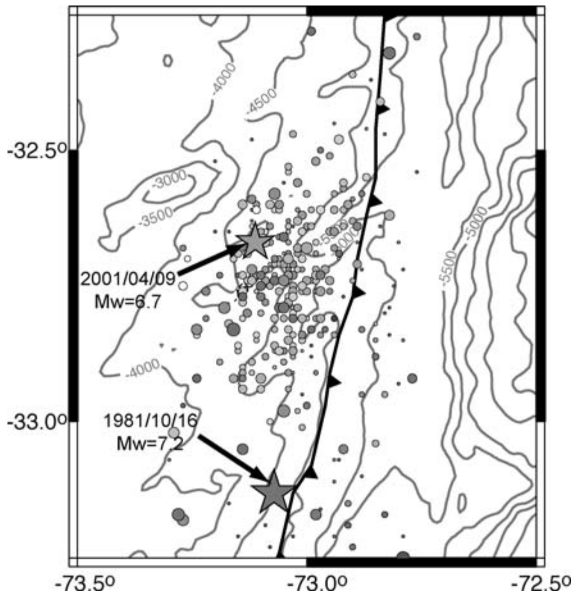

Figure 2. ISC seismicity of the region outlined in the box of Figure 1. The two largest earthquakes, which occurred on 16 October 1981 (M_w 7.2) and 9 April 2001 (M_w 6.7), are shown by stars.

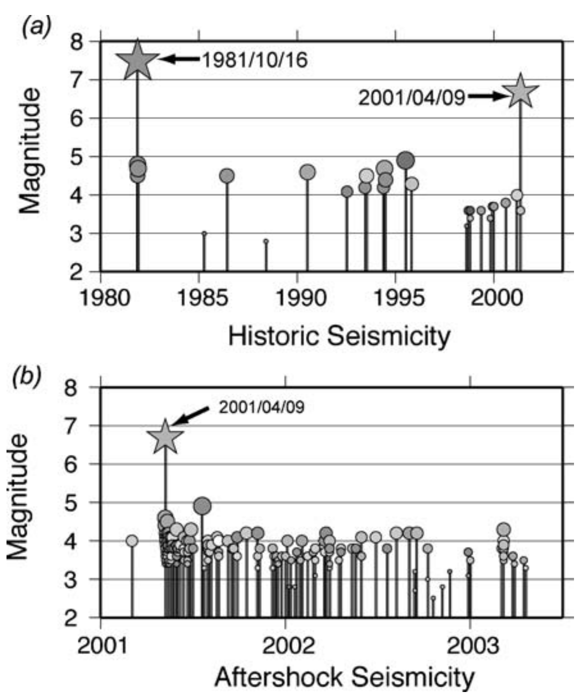

Figure 3. (a) Historic ISC seismicity of the outer-rise region within the box outlined in Figure 1 from 1980 to the 9 April 2001 mainshock in this study. (b) Seismicity from 2001 to 2004 showing aftershocks of the 9 April 2001 earthquake.

Table 1. Velocity structure used for the regional moment tensor inversion. A structure given by the Preliminary Reference Earth Model (PREM) (Dziewonski and Anderson, 1981) was assumed beneath the upper mantle.

Layer	Thickness (km)	P-wave velocity (km/s)	S-wave velocity (km/s)
Crust	34	5.90	3.27
Upper mantle	45	7.81	4.11
Deeper	PREM	PREM	PREM

Moment tensor inversion

Using the broadband waveforms recorded at five stations of the CHARGE network (Figure 1), we obtained the regional moment tensor for the mainshock on 9 April 2001. The least square regional moment-tensor inversion (RMTI) technique consists of fitting observed band-pass filtered waveforms with synthetic seismograms using a seismic velocity structure for a fixed source depth (Randall et al., 1995). To obtain the best solution we repeated the inversion for many trial depths after testing for the optimal band-pass filter that in practice also depends on the magnitude of the event. We use the entire waveform on all three seismic displacement components using a band-pass between 50 and 100 second. In this case, the seismic velocity structure is particularly complex along the expected ray paths. Hence, we compared synthetic and observed data aligned at the first P-wave arrival for each station to reduce the dependence on the chosen structure, origin-time and location uncertainties. We also used the longer periods to decrease the dependence on the crustal seismic velocity structure, limiting the number of stations to those with STS2 sensors (labeled stations in Figure 1). We obtained the double-couple focal mechanisms for a series of fixed depths between 3 and 27 km (Figure 4) using the simple 1D seismic velocity structure described in Table 1. In addition, we tested other seismic models and show examples in Figure 4b. This figure shows the results of our preferred model in Table 1 using a small perturbation to the crustal P-wave velocity (Vp = 6.1 km/s) (Model a) and to the upper-mantle S-wave velocity (Vs = 4.19 km/s) (Model b). Note how stable the focal mechanism solution is for the range of tested models.

The focal parameters are summarized in Table 2 and agree well with the extensional Harvard CMT solution. A range of depths less than 12 km produced similar

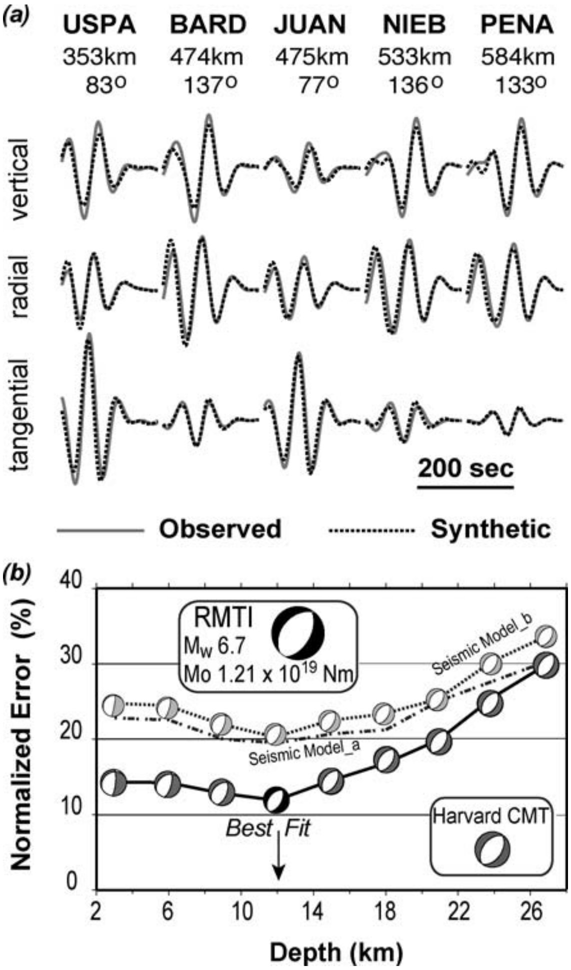

Figure 4. Results of the regional moment tensor inversion (RMTI). (a) Observed and synthetic band-pass filtered (0.01–0.02 Hz) displacement waveforms for the stations shown in Figure 1. The numbers below station names correspond to the epicentral distance and azimuth for each station. (b) Depth dependence of the normalized synthetic to observed amplitude misfit and the focal mechanism. The best fit is found at 12 km depth. Also shown are the results using different seismic models (see text). Only some focal mechanisms are plotted for simplicity. The Harvard CMT solution is shown for reference.

focal mechanisms with normalized misfit errors below 15%. At depths greater than 12 km the synthetic seismograms showed increased misfit to the observed data (Figure 4b).

Aftershock relocation

Aftershock distributions are often used as proxies for rupture areas. Considering the problems in obtaining accurate hypocentral locations using traditional

Table 2. Comparison between Regional Moment Tensor Inversion (RMTI), Harvard CMT, NEIC and ISC catalog information for the 9 April 2001 outer-rise earthquake

Head	RMTI	CMT	NEIC	ISC
Strike	29°/222°	33°/219°		
Dip	51°/39°	46°/44°		
Rake	−98°/−80°	−94°/−86°		
Longitude		73.23°W	73.11°W	73.11°W
Latitude		32.88°S	32.67°S	32.66°S
Depth (km)	<12	15	11	11
Seismic moment M_0 (Nm)	1.21×10^{19}	1.17×10^{19}		

methods caused by uncertainties in the velocity structure, different relocation techniques have been developed over time. Most of them assume that the travel path is much longer than the relative distance between two or more events. Using differential travel times eliminates the effect of inaccurate structure, improving significantly the quality of relative positioning of the events. In this study, we used the double-difference relocation technique HypoDD, since it was developed for strongly clustered event groups observed at regional distances (Waldhauser and Ellsworth, 2000).

Figure 5a shows a map of the 142 relocated events using a total of 2633 regional P- and S-phase arrivals. The arrival times were obtained from the ISC catalog for the permanent stations and by handpicking events of magnitude >4 on the temporary broadband stations. It should be noted that during the convergence of HypoDD, the algorithm discards events that fail to remain clustered, explaining why only 142 could be relocated. The discarded events do not show any systematic pattern in magnitude or location, suggesting that the resulting earthquake locations are not biased due to artifacts of the relocation process. The results show that the mainshock was located at 10 km depth and that aftershocks occurred within a depth range of 10–30 km. The average relative errors are 3 km, 1.5 km and 3.5 km in the E-W, N-S and vertical component, respectively. For each component, 90% of the events have relative errors smaller than 5 km. Different seismic structures affect mainly the relocated depth but do not change their relative relocation in the cluster. Thus even if the mainshock epicenter is moved to the uppermost oceanic crust, the aftershocks still occur downward in the lithosphere (Figures 5 and 6).

To study the geometry of the relocated earthquakes, we performed a principal-component analysis (PCA)

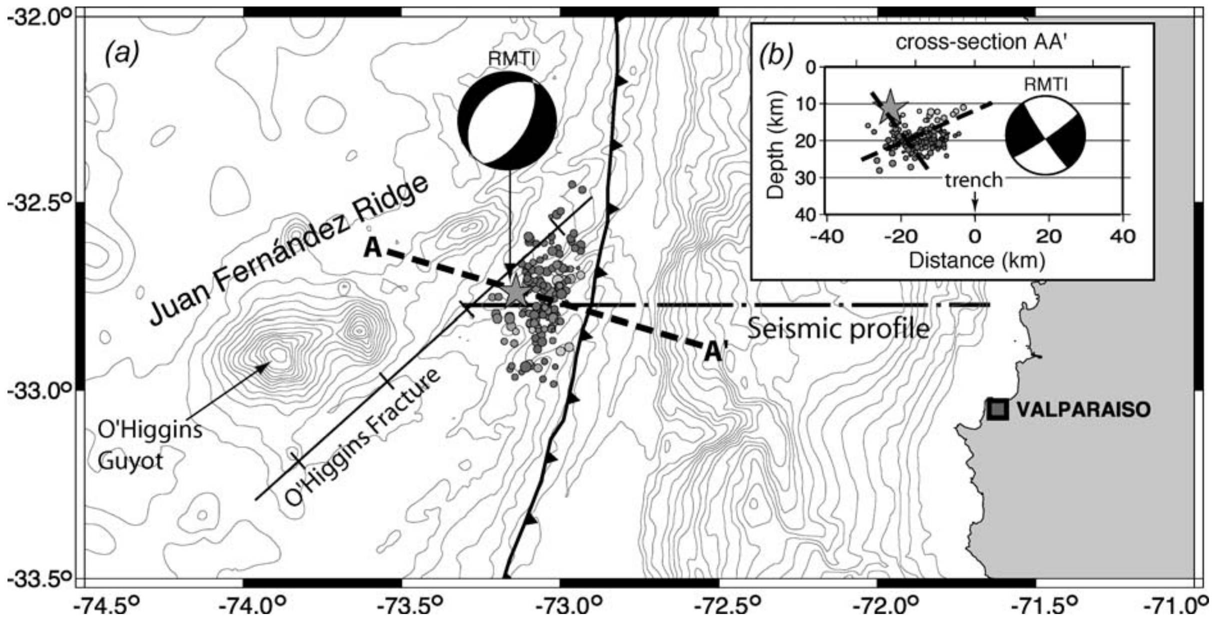

Figure 5. (a) Map view of the relocated seismicity using HypoDD. The lower hemisphere projection focal mechanism corresponds to the regional moment tensor inversion (RMTI) shown in Figure 4. Profile AA′ is chosen perpendicular to the direction of the largest principal component (see text) and is also roughly perpendicular to the strike of the focal mechanism and the trench. The long dashed line shows the seismic profile location from Flueh et al. (1998). The O'Higgins fracture is taken from van Huene et al. (1997). (b) Cross section along profile AA′. The azimuth of the profile and the dip of the two dashed lines in the cross section were computed from a principal-component analysis. The focal mechanism is also shown as a vertical plane projection.

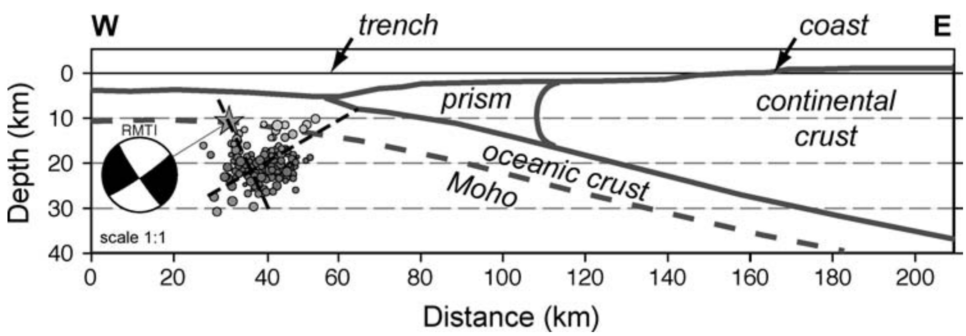

Figure 6. Cross section of the relocated outer-rise seismicity, focal mechanism, dip of in-plane principal components and crustal thickness according to the seismic profile (see location in Figure 5) modified from Flueh et al. (1998).

(Davis, 1973). The results suggest, in order of importance, that a roughly N-S trending horizontal axis (azimuth of 9°) explains 72% of the variance and that two perpendicular secondary axes dipping 30° to the west and 60° to the east explain the remaining 18% and 10% of the variance, respectively. The direction of the first horizontal axis can be explained by the relatively wide N-S distribution of the aftershocks (Figure 5a), while the two secondary directions are caused by the apparent clustering along the two dipping planes, which correlate well with the fault plane dips of 51° to the east and 39° to the west predicted by our RMTI solution (see Table 1). This indicates an apparent spatial correlation of the focal mechanism and aftershock distribution (Figure 5b), suggesting, in conjunction with the location of the mainshock, that the actual rupture plane corresponds to the steeper-dipping focal plane.

Discussion

To visualize the location of the earthquakes in the context of the local structures, we plotted a cross section of the relocated seismicity over the seismic profile modified from Flueh et al., (1998) (Figures 5 and 6). The depth of the mainshock determined by both the waveform modeling and the aftershock relocation is consistent and seems to be located within or at least near the bottom of the seismically imaged oceanic crust at 10–12 km. The relocated aftershock distribution extends ~70 km in the NS direction and is confined within a depth range of 10–30 km, suggesting that the rupture propagated into the oceanic lithosphere for at least 20 km. The seismic moment of 1.21×10^{19} Nm and the rupture area defined by the aftershock distribution yield an average coseismic displacement of 0.5–1.0 m. This slip is consistent with an earthquake of this magnitude, indicating that the rupture area is consistent with the size of the mainshock. The maximum depth to which the co-seismic rupture propagated is hard to constrain. Aftershock depths suggest brittle failure to 30 km, but this might reflect the transition level of a brittle (i.e., seismogenic) to a more ductile (i.e., aseismic) rheology and not the mainshock rupture depth. However, assuming that the elastic strength of the whole lithosphere is predominantly supported by the brittle layer, it is possible to speculate that the mainshock broke the whole effective thickness of the lithosphere. The absence of aftershocks above the mainshock could be explained by the overlying weak sediment layer or by hydrated oceanic crust, conditions that allow an initiated rupture to propagate to the surface but prevent seismicity from nucleating and hence aftershocks. The secondary conjugate aftershock plane indicates a similar behavior, where aftershocks occur only in the lower oceanic crust and lithosphere.

Further, the tensional source mechanism of the mainshock and the apparent alignment of the aftershocks along two perpendicular planes dipping 60°E and 30°W, where one of them is consistent with one nodal plane of the mainshock focal mechanism, indicates the activation of the secondary conjugate fault plane. Moreover, the strike orientations of the fault planes are well aligned with the nearby O'Higgins Fracture scarp discovered by high-resolution bathymetric swath mapping (von Huene et al., 1997; Kopp et al., 2004) (see Figure 5a). In conjunction with the seismic evidence, the 110-km-long fracture that trends parallel to the Juan Fernández Ridge can be interpreted as the surface manifestation of a large normal fault system (Kopp et al., 2004), whose northeastern segment might have ruptured during the 9 April 2001 event. This suggests that the ridge plays a mayor role in the nucleation of outer-rise seismicity and therefore controls the stress state near the trench. The alignment of aftershocks along planes extending down into the mantle suggests that the fractures observed at the surface might be of lithospheric scale, hence acting as a natural conduit for hydration of the oceanic mantle as inferred by Kopp et al., (2004) based on low mantle seismic velocities.

The distribution of shallow outer-rise seismicity along the Chilean margin (Figure 7) further supports this hypothesis. With the exception of the potential outer-rise seismicity south of 34–35°S, which is very likely a post-seismic response of the anomalously

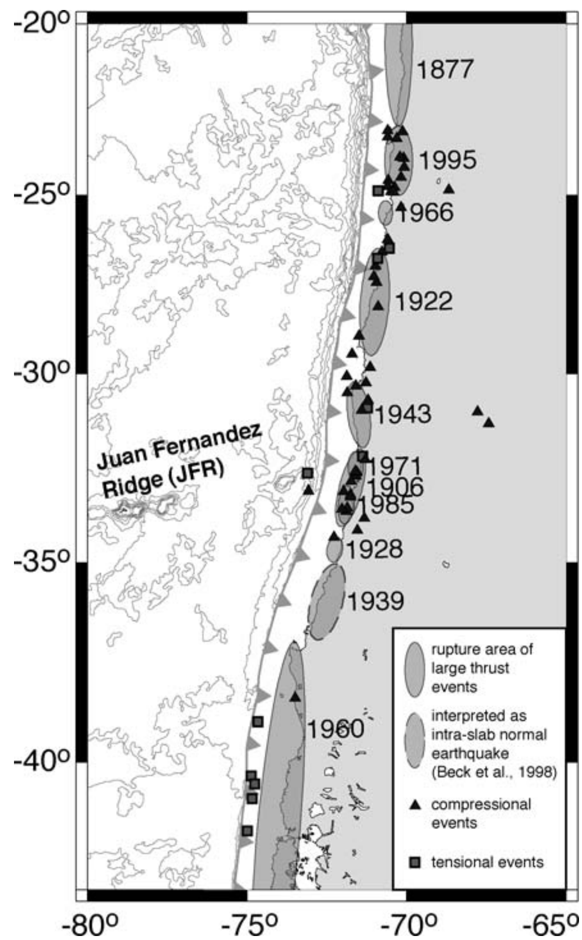

Figure 7. Map of the South American western margin showing rupture areas of large underthrust earthquakes (Beck et al., 1998) and shallow source mechanisms given by the Harvard CMT catalog from 1977 to 2002 ($M_w > 6.0$ and depths <70 km).

large thrust event of 1960 (M_w 9.6) (Christensen and Ruff, 1988; Lay et al., 1989), the outer-rise along the Chilean margin has produced large events only in the vicinity of the collision of the Juan Fernández Ridge with the trench. North of 33°S, where no significant bathymetric features subduct beneath the South American plate, the absence of outer-rise seismicity implies no correlation with large interplate events. Of course, we cannot rule out a bias introduced by mislocated events or the limited historical network coverage.

The occurrence of the 1981 (M_w 7.2) compressional event in the vicinity of our study remains to be explained. The depth of this event is somewhat controversial (Christensen and Ruff, 1985; Honda et al., 1990; Tichelaar et al., 1992), but it is generally accepted that it occurred at depths of 20–40 km, deeper than the typical extensional outer-rise seismicity. This can be explained by bending stresses below the neutral surface (Chapple and Forsyth, 1979) or by a time-dependent compressional loading of the outer-rise caused by the locking of the interplate contact zone prior to the large (M_w 8.0) thrust event that occurred on 3 March 1985 near the coast of Valparaiso (Christensen and Ruff, 1988).

The absence of outer-rise seismicity along the northern segment of the margin suggests that in either case, a reactivation of the preexisting normal structures (possibly in the reverse direction for compressional events) is required to allow outer-rise events to occur, thus explaining why the only two large outer-rise events that have occurred in the last 40 years are associated with the subduction of the Juan Fernández Ridge. The only exception is the outer-rise seismicity observed offshore of the rupture area of the large 1960 earthquake, which, considering the anomalous magnitude of that event, may represent an anomaly in the normal outer-rise dynamics active along the rest of the margin.

Two moderate tensional outer-rise earthquakes are also reported in the Harvard CMT catalog near the Nazca Ridge and the Nazca Fracture Zone collision further north at ∼16°S along this convergent margin. Both bathymetric subducting features are characterized by normal faults (Hampel et al., 2004). Based on this evidence it is possible that these major bathymetric features have some effect on the reactivation of local faults that generate outer-rise seismicity. However, without a detailed study of the locations of these two events we hesitate to speculate about their connection to bathymetric features.

Conclusions

A combination of regional permanent and PASSCAL portable seismic networks in Chile and Argentina, consisting of short-period and broadband stations, provide a valuable tool for a detailed study of the seismicity of the off-shore region. By combining the large number of travel-time picks and the high-quality broad-band records we were able to constrain the source mechanism and depth of the 2001 mainshock and its associated aftershock sequence. We can summarize our conclusions in the following points:

1. The mainshock has a normal source mechanism striking approximately parallel to the Juan Fernández Ridge and its associated structures (O'Higgins Fracture), suggesting that ridge-related preexisting structures play a predominant role in outer-rise seismic nucleation compared to the flexural bending caused by the subduction initiated at the trench.
2. Dip angles of the focal planes of the mainshock correlate well with the distribution of the aftershocks along two perpendicular planes, suggesting the activation of a conjugate normal fault system.
3. The extension of the seismicity below the crust suggests the existence of possibly lithospheric-scale fault systems which may act as natural conduits to hydrate the oceanic mantle.
4. With the exception of very large interplate events, along the Chilean margin the existence of preexisting fractures may be required to generate outer-rise seismicity.

Acknowledgments

We acknowledge the comments of two anonymous reviewers. We thank Norm Meader for his help to improve this manuscript. This work was supported by NSF grant EAR9811870. Seismic data were acquired at stations provided by the IRIS/PASSCAL program. We would like to thank the Seismological Service of the University of Chile for providing us with their seismic catalog and the National University of San Juan and Instituto Nacional de Prevención Sísmica (INPRES) in Argentina.

References

Beck, S., Barrientos, S., Kausel, E. and Reyes, M., 1998, Source characteristics of historic earthquakes along the central Chile subduction zone, *J. South American Earth Sci.* **11**(2), 115–129.

Brooks, B.A., Bevis, M., Smalley Jr., R., Kendrick, E., Manceda, R., Lauria, E., Maturana, R. and Araujo, M., 2003, Crustal motion in the southern Andes (26°–36°S): Do the Andes behave like a microplate? *Geochem. Geophys. Geosystem.* **4**, 1–14.

Cahill, T.A. and Isacks, B.L., 1992, Seismicity and shape of the subducted Nazca Plate, *J. Geophys. Res.* **97**(B12), 17, 503–17, 529.

Chapple, W.M. and Forsyth, D.W., 1979, Earthquakes and bending of plates at trenches, *J. Geophys. Res.* **84**(B12), 6729–6749.

Christensen, D.H. and Ruff, L.J., 1983, Outer-rise earthquakes and seismic coupling, *Geophys. Res. Lett.* **10**(8), 697–700.

Christensen, D.H. and Ruff, L.J., 1985, Analysis of the trade-off between hypocentral depth and source time function, *Bull. Seismol. Soc. Am.* **75**(6), 1637–1656.

Christensen, D.H. and Ruff, L.J., 1988, Seismic coupling and outer rise earthquakes, *J. Geophys. Res.* **93**(B11), 13421–13444.

Davis, J.C., 1973, *Statistics and Data Analysis in Geology*, John Wiley & Sons.

Dziewonski, A.M. and Anderson, D.L., 1981, Preliminary reference Earth model, *Physic. Earth Planet. Interiors* **25**(4), 297–356.

Flueh, E.R., Vidal, N., Ranero, C.R., Hojka, A., Huene, R. von, Bialas, J., Hinz, K., Cordoba, D., Danobeitia, J.J. and Zelt, C., 1998, Seismic investigation of the continental margin off- and onshore Valparaiso, Chile, *Tectonophysics* **288**(1–4), 251–263.

Forsyth, D., 1982, Determinations of focal depths of earthquakes associated with the bending of oceanic plates at trenches, *J. Geophysic. Res.* **87**(B8), 6853–6864.

Hampel, A., Kukowski, N., Bialas, J., Huebscher, C. and Heinbockel, R., 2004, Ridge subduction at an erosive margin: The collision zone of the Nazca Ridge in southern Peru, *J. Geophys. Res.* **109**, B02101, doi:10.1029/2003JB002593.

Honda, S., Kawakatsu, H. and Seno, T., 1990, The depth of the October 1981 off Chile outer-rise earthquake (Ms=7.2) estimated by a comparision of several waveform inversion methods, *Bull. Seismol. Soc. Am.* **80**(1), 69–87.

Huene, R. von, Corvalán, J., Flueh, E.R., Hinz, K., Korstgard, J., Ranero, C.R., Weinrebe, W. and CONDOR Scientists, 1997, Tectonic control of the subducting Juan Fernández Ridge on the Andean margin near Valparaiso, Chile, *Tectonics* **16**(3), 474–488.

Kanamori, H., 1971, Seismological evidence for a lithospheric normal faulting – the Sanriku earthquake of 1933, *Physic. Earth Planet. Interiors* **4**, 249–300.

Kopp, H., Flueh, E.R., Pepenberg, C. and Klaeschen, D., 2004, Seismic investigations of the O'Higgins Seamount Group and the Juan Fernández Ridge: aseismic ridge emplacement and lithosphere hydration, *Tectonics* **23** (TC2009), doi:10.1029/2003TC001590.

Lay, T., Astiz, L., Kanamori, H. and Christensen, D.H., 1989, Temporal variation of large intraplate earthquakes in coupled subduction zones, *Physic. Earth Planet. Interiors* **54**(3–4), 258–312.

Mueller, S., Choy, G.L. and Spence, W., 1996a, Inelastic models of lithospheric stress – I. Theory and application to outer-rise plate deformation, *Geophysic. J Int.* **125**(1), 39–53.

Mueller, S., Spence,W. and Choy, G.L., 1996b, Inelastic models of lithospheric stress – II. Implications for outer-rise seismicity and dynamics, *Geophysic. J. Int.* **125**(1), 54–72.

Randall, G.E., Ammon, C.J. and Owens, T.J., 1995, Moment tensor estimation using regional seismograms from a Tibetan Plateau portable network deployment, *Geophys. Res. Lett.* **22**(13), 1665–1668.

Stauder, W., 1968a, Mechanism of the Rat Island earthquake sequence of February 4, 1965, with relation to island arcs and sea-floor spreading, *J. Geophys. Res.* **73**(B12), 3847–3858.

Stauder, W., 1968b, Tensional character of earthquake foci beneath the Aleutian trench with relation to sea-floor spreading, *J. Geophys. Res.* **73**(B24), 7693–7701.

Tichelaar, B.W., Christensen, D.H. and Ruff, L.J., 1992, Depth extend of rupture of the 1981 Chilean outer-rise earthquake as inferred from long-period body waves, *Bull. Seismol. Soc. Am.* **82**(3), 1236–1252.

Waldhauser, F. and Ellsworth, W.L., 2000, A double-difference earthquake location algorithm: Method and application to the northern Hayward fault, California, *Bull. Seismol. Soc. Am.* **90**(6), 1353–1368.

Yañez, G., Ranero, C.R., Huene, R. von and Diaz, J., 2001, Magnetic anomaly interpretation across the southern central Andes (32°–34°S): The role of the Juan Fernández Ridge in the late Tertiary evolution of the margin, *J. Geophys. Res.* **106**(B4), 6325–6345.